J Supercond Nov Magn (2010) 23: 1511–1516
DOI 10.1007/s10948-010-0805-x

ORIGINAL PAPER

Temperature Dependence of the Intergranular Critical Current Density in Uniaxially Pressed $Bi_{1.65}Pb_{0.35}Sr_2Ca_2Cu_3O_{10+\delta}$ Samples

I. García-Fornaris · A.A. Planas · P. Muné · R.F. Jardim · E. Govea-Alcaide

Received: 13 April 2010 / Accepted: 3 June 2010 / Published online: 23 June 2010

Abstract We have studied the normal and superconducting transport properties of $Bi_{1.65}Pb_{0.35}Sr_2Ca_2Cu_3O_{10+\delta}$ (Bi-2223) ceramic samples. Four samples, from the same batch, were prepared by the solid-state reaction method and pressed uniaxially at different compacting pressures, ranging from 90 to 250 MPa before the last heat treatment. From the temperature dependence of the electrical resistivity, combined with current conduction models for cuprates, we were able to separate contributions arising from both the grain misalignment and microstructural defects. The behavior of the critical current density as a function of temperature at zero applied magnetic field, $J_c(T)$, was fitted to the relationship $J_c(T) \propto (1 - T/T_c)^n$, with $n \approx 2$ in all samples. We have also investigated the behavior of the product $J_c\rho_{sr}$, where ρ_{sr} is the specific resistance of the grain-boundary. The results were interpreted by considering the relation between these parameters and the grain-boundary angle, θ, with increasing the uniaxial compacting pressure. We have found that the above type of mechanical deformation improves the alignment of the grains. Consequently the samples exhibit an enhance in the intergranular properties, resulting in a decrease of the specific resistance of the grain-boundary and an increase in the critical current density.

I. García-Fornaris · A.A. Planas
Departamento de Ciencias Básicas, Universidad de Granma, Apdo. 21, P.O. Box 85100, Bayamo, Cuba

P. Muné · E. Govea-Alcaide (✉)
Departamento de Física, Universidad de Oriente, Patricio Lumumba s/n, P.O. Box 90500, Santiago de Cuba, Cuba
e-mail: malvareza@udg.co.cu

R.F. Jardim
Instituto de Física, Universidade de São Paulo, CP 66318, 05315-970 São Paulo, SP, Brazil

Keywords Bi-based superconductors · Degree of texture · Weak links · Electrical conductivity

1 Introduction

The study of the temperature dependence of the critical current density, $J_c(T)$, in high-T_c polycrystalline superconductors has interest from the practical and from the purely fundamental point of view. For practical applications, the target is to improve and/or optimize the electrical properties of the materials, mostly across grain-boundaries which are regions of mismatch between grains with misoriented crystalline axes. On the other hand, the challenge in the fundamental studies is to better understand the transport mechanisms in both within the grains or across the grain-boundaries. In granular materials, the transport properties strongly depend on their microstructures, being the individual grains and the grain-boundaries the most important structural units [1]. Various models have been employed to explain the behavior of the $J_c(T)$ dependence in a wide range of temperatures [2]. The behavior of the intragrain component, $J_{cg}(T)$, can be explained by the Anderson–Kim flux-creep critical-state model or by the Ginzburg and Landau model [2, 3]. The intergrain $J_c(T)$ is usually interpreted using theories developed by Ambegaokar and Baratoff model [3] or Ambegaokar and Halperin model [4] (which is based on the thermally activated phase-slippage). It is important to point out that most of these models have been developed for a single junction and generally, the $J_c(T)$ dependence follows a power law of the type $J_c(T) \propto (1 - T/T_c)^n$, where T_c is the superconducting critical temperature and n is an exponent, in which values usually are found in the 1–2.5 interval [2, 4–6]. Regarding

the temperature dependence of J_c some authors have reported, depending of the sample type (bicrystal, thin-film or bulk), a value of $n = 2$ is consistent with Likharev's model which predicted for dirty superconductor–normal-metal–superconductor junctions (SNS) [1, 2, 5]. In contrast, for $n = 1.5$ the experimental data is usually described in terms of the Ambegaokar–Baratoff's theory for superconductor–insulator–superconductor junctions (SIS) [2]. However, the application of these single-junction models to granular materials is not a simple task because according to the preparation process these samples exhibit a wide variety of junction types. Moreover, depending on the temperature range in given a sample the value of n can manifest different crossovers, which also can be induced by using a dc applied magnetic field [2].

On the other hand, it is well established that the mismatch between adjacent grains, with misoriented crystalline axes, are very effective into depress the superconducting order parameter at grain-boundaries and to suppress the supercurrent across physical grains. Such a statement has support in studies of single, artificially fabricated grain-boundaries, where J_c of a grain-boundary junction depends exponentially on the misorientation angle [7, 8].

In previous works, we have shown that ceramics samples of $Bi_{1.65}Pb_{0.35}Sr_2Ca_2Cu_3O_{10+\delta}$ (Bi-2223) with similar intragranular properties, but different intergranular features can be obtained by using different values of the uniaxial compacting pressures before the last heat treatment [9, 10]. (In this work we present measurements) of the intergranular transport properties in that uniaxially pressed $Bi_{1.65}Pb_{0.35}Sr_2Ca_2Cu_3O_{10+\delta}$ (Bi-2223) ceramic samples. We have concentrated efforts in extract relevant information concerning the intergranular properties of these samples from measurements of the electrical resistivity as a function of temperature, $\rho(T)$, and the transport critical current density as a function of temperature, $J_c(T)$, in temperatures very close to T_c. Also, other characterizations were conducted to analyze the microstructural behavior of samples.

2 Experimental Procedure

Polycrystalline samples of $Bi_{1.65}Pb_{0.35}Sr_2Ca_2\ Cu_3O_{10+\delta}$ (Bi-2223) were prepared from powders of Bi_2O_3, PbO, $SrCO_3$, $CaCO_3$, and CuO, which were mixed in an atomic ratio of Bi:Pb:Sr:Ca:Cu (1.65:0.35:2:2:3). The mixture was first calcined in air at 750 °C for 40 h. Then, the powder was reground and pressed into pellets of 10 mm in diameter and 2 mm in thickness at a pressure of 120 MPa. These pellets were heat treated at 800 °C in air for 40 h. Subsequently, the samples were reground, pressed again, and sintered in air at 845 °C for 40 h. This step was repeated three times, as described elsewhere [10, 11]. Finally, the pellets were reground and the obtained powders were uniaxially pressed at different compacting pressures ranging from 100 to 250 MPa (see Table 1). The typical dimensions of the pellets were $d = 15$ mm in diameter and $h = 1$ mm in height. The last heat treatment was performed in air at 845 °C for 40 h followed by slow cooling.

We have evaluated the phase identification in both powder and bulk samples from the X-ray diffraction patterns obtained in a Bruker-AXS D8 Advance diffractometer. These measurements were performed at room temperature using Cu Kα radiation in the $3° \leq 2\theta \leq 80°$ range with a 0.05° (2θ) step size, and 5 s counting time.

The morphology of grains in a powder sample was observed by using a JEOL JSM-5800 scanning electron microscope operated at 25 kV. From this type of micrography we were able to estimate the mean size of the grains in our samples.

Two types of transport measurements were performed: (i) the temperature dependence of the electrical resistivity, $\rho(T)$, and (ii) the current–voltage (I–V) for different temperatures. These measurements were performed in a closed cycle cryogenics refrigerator ARS-4HW/DE-202N attached to a temperature controller Lakeshore model 331S.

The temperature dependence of the electrical resistivity, $\rho(T)$, in the temperature range $77\ \text{K} \leq T \leq 300\ \text{K}$ was measured by using the standard dc four-probe technique. Before each measurement, the samples were cooled from room temperature down to 77 K. Then, an excitation current, $I = 1$ mA, was injected along the major length of the samples. The voltage across the sample and the temperature were both collected while the temperature was raised slowly to 300 K. The typical dimensions of samples were $t = 1$ mm (thickness), $w = 2$ mm (width), and $l = 10$ mm (length).

On the other hand, experimental I–V measurements were also performed by using the standard dc four-probe technique. After cooling the sample in zero applied magnetic field to a certain temperature T, the excitation current through the sample is increased automatically in steps of 1 mA, while the voltage across the sample is measured. Under these circumstances, we have extracted the value of the transport critical current at zero applied magnetic field, $I_c(0)$, from the measured I–V curve, by taking the I_c value as the I in which the voltage across the sample reaches 1 μV. The above procedure is repeated several times for different fixed values of T in order to construct the transport critical current curve as a function of temperature, $I_c(T)$.

3 Results and Discussion

The X-ray diffraction patterns, taken on bulk samples showed that all samples have similar chemical composition

Table 1 Relevant parameters of the samples studied in this work: compacting pressure, the linear slope A of $\rho(T)$, the residual resistivity $\rho(0)$ at $T = 0$, the intergranular electrical resistivity ρ_{wl}, the effective area factor α_n. We have also included parameters obtained from the fitting procedure for $J_c(T)$ data to the relation $J_c(T) \propto (1 - T/T_c)^n$, the critical temperature and the exponent n. Finally, values of the product $J_c\rho_{sr}$ at $T = 0.96T_c$ are also reported

Sample	P (MPa)	A (μΩ cm/K)	$\rho(0)$ (mΩ cm)	ρ_{wl} (mΩ cm)	α_n	T_c (K)	n	$J_c\rho_{sr}$ ($\times 10^{-3}$ mV)
BP2	99	12.59	2.54	0.37	0.15	107.0	2.41	4.2
BP3	148	9.75	1.06	0.20	0.19	108.5	1.93	9.2
BP4	198	8.98	0.90	0.18	0.20	109.1	1.96	14.4
BP5	247	7.92	0.76	0.17	0.23	109.5	2.04	21.8

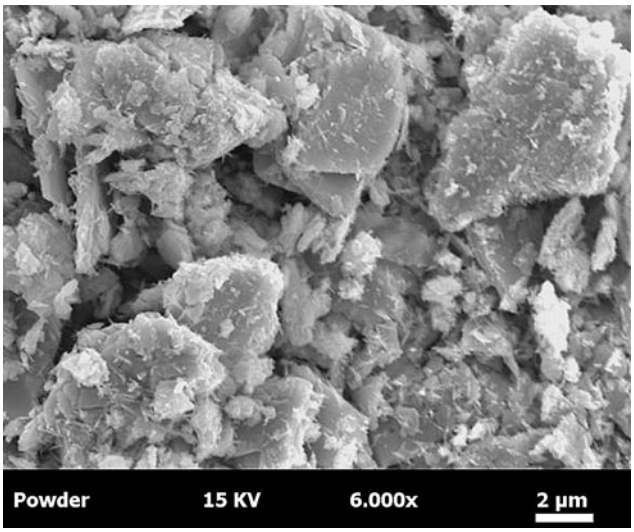

Fig. 1 Typical SEM images used to study the morphology and to estimate the average grain size. This micrograph was taken on powders of the sample BP2

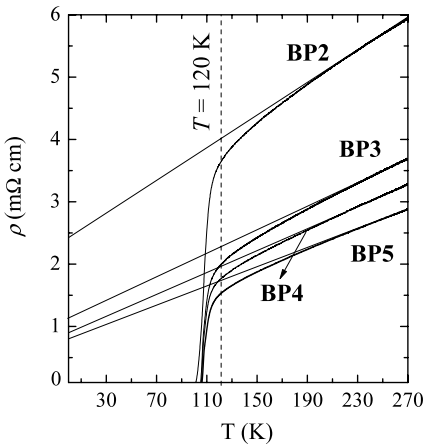

Fig. 2 Temperature dependence of the electrical resistivity of samples BP2, BP3, BP4, and BP5

and their indexed reflections are related to the high-T_c Bi-2223 phase [9, 11]. The unit-cell parameters were calculated regarding an orthorhombic unit cell and the obtained values $a \approx b = 5.41$ Å, and $c = 37.15$ Å are in line with those reported elsewhere for the same compound [12–14]. The occurrence of grains with platelet-like structure in Bi-based materials is well known [9, 11]. Figure 1 shows a micrograph taken on powders of the sample BP2 that was reground after the last heat treatment. At first glance, the morphology of grains is very similar. The occurrence of grains with platelet-like structure is a signature of the Bi-2223 phase formation from the Bi-2212 matrix [11]. The average grain size was found to be $L_a \sim 4$ μm long and $L_c \sim 0.5$ μm thick. This kind of morphology along with the compacting pressure allow the orientation of the grains with their c-axes ((00l) crystallographic planes) parallel to the compacting direction. Rocking curves were conducted in these samples for gaining information about the degree of texture of the grains and the obtained results demonstrate the better alignment of grains with increasing the uniaxial compacting pressure [15].

All the samples were also characterized by measurements of electrical resistivity versus temperature $\rho(T)$. Figure 2 displays the $\rho(T)$ curves of samples BP2, BP3, BP4, and BP5. A careful inspection of the data indicates that curves exhibit a transition to the superconducting state bellow the so-called onset superconducting critical temperature $T_{on} \sim 120$ K. However, the temperature in which the zero resistance state is observed, T_{off}, increases from 98 K (BP2) to 105 K (BP5). For temperatures above T_{on}, the $\rho(T)$ curves exhibit a clear metallic-like behavior. As the onset temperature is related to the transition of the isolated grains to the superconducting state then its constant value in all samples strongly suggests that the grains have similar stoichiometry. This result is in excellent agreement with those of XRD. On the other hand, T_{off} is related to volume fraction of the Bi-2223 phase and/or features of the intergranular component. Thus, as the chemical composition of grains are similar then the observed behavior of the offset temperature is just related to differences in the intergranular properties between samples [9, 11].

Relevant information regarding the intergranular features of the samples can be extracted from the $\rho(T)$ data by using a conduction model described in details elsewhere [16]. In such a model, the $\rho(T)$ data is described by the equation:

$$\rho(T) = \frac{1}{\alpha_n}\big(\rho_{ab}(T) + \rho_{wl}\big), \tag{1}$$

where α_n is given by

$$\alpha_n = f\alpha_{srt}, \tag{2}$$

and represents an effective area factor related to contributions of: (i) the misalignment of the grains and/or the degree of texture which is given by f $(0 < f \leq 1)$ and (ii) microstructural defects such as voids and microcracks which is related to α_{str} $(0 < \alpha_{str} \leq 1)$. In such a model, the grains are believed to (behave as single crystals). This implies that the first term in (1), ρ_{ab}, is related to the average of the electrical resistivity along the ab-plane. Such a contribution, in our analysis, has been assumed to be linearly temperature dependent and with slope $A_{sc} = 1.84$ μΩ cm/K, a value extracted from the $\rho(T)$ data in Bi-2223 single crystals [17, 18]. The model also assumes zero-residual temperature intercept [16, 17]. The term ρ_{wl} in (1) is regarded as the average intergranular electrical resistivity, assumed to be temperature-independent. The parameters α_n and ρ_{wl} were obtained by fitting the $\rho(T)$ data to the typical linear dependence $\rho(T) = AT + \rho(0)$ along with the expressions [16]:

$$\alpha_n = \frac{A_{sc}}{A}, \tag{3}$$

and

$$\rho_{wl} = \alpha_n \rho(0), \tag{4}$$

where A is the slope of the $\rho(T)$ curve in the T-linear region, and $\rho(0)$ the residual resistivity at $T = 0$ (see Table 1). We want to remark that in this model the effects of misalignment between grains and structural defects are included in α_n. Within the experimental conditions, errors in determining α_n and ρ_{wl} are close to 10%. After these corrections the *resulting sample* behaves as a grain-aligned equivalent sample with reduced cross section and increased length. In this case the excitation current crosses the sample through parallel and independent channels [16, 19]. Under these conditions, is permissible to rewrite the intergranular electrical resistivity in terms of the normal-state resistance of the average junction, R_{wl}, as $\rho_{wl} = R_{wl}L_a$ [19]. Notice that ρ_{wl} is different from the specific resistance of a single grain-boundary, $\rho_{sr} = R_{wl}A^2$, where A is the cross-sectional area of the junction [19]. If we consider that grains of Bi-2223 samples have a platelet-like structure then $A = L_a L_c$, which according to the SEM micrograph (see Fig. 1) in our samples $A \approx 2 \times 10^{-8}$ cm^2.

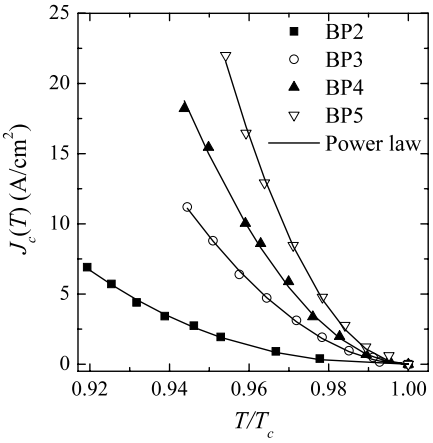

Fig. 3 Critical current density as a function of the reduced temperature for samples BP2, BP3, BP4, and BP5. *Solid lines* represent fitting to the power law $J_c(T) \propto (1 - T/T_c)^n$ with $n \sim 2$, as reported in Table 1

As displayed in Table 1, the observed rise of α_n with increasing compacting pressure is certainly related to both the increasing degree of texture and the decrease of the influence of microstructural defects to $\rho(T)$. Under this circumstance, see (3), the decrease of ρ_{wl} between samples BP2 (0.37 mΩ cm) and BP5 (0.17 mΩ cm) agrees well with the previous statement. However values of the intergranular electrical resistivity between samples BP4 and BP5 are essentially the same indicating that intergranular properties of these samples are identical. Additionally, estimations of ρ_{sr} yield values in the range 10^{-7}–10^{-8} Ω cm^{-2}, which also imply normal-state resistances $R_{wl} = 0.93$ Ω, for the sample BP2, and $R_{wl} = 0.43$ Ω for BP5. Values reported above are within the expected range for these parameters [20, 21]. Also, the above results strongly suggests that grain-boundaries in our samples behaves as superconductor–normal-metal–superconductor (SNS) junctions [1, 5].

We have also measured the superconducting critical current density as a function of the reduced temperature, $t = T/T_c$. The results for samples BP2, BP3, BP4, and BP5 are shown in Fig. 3. Noticeable that all curves exhibit a similar qualitative behavior. Also, we have fit these experimental data to a power law of the type $J_c(T) \propto J_c(0)(1 - T/T_c)^n$, where n is an exponent [1, 5]. The obtained results shown that n assumes a value close to 2.4 for sample BP2 and exhibits a certain tendency to 2 in samples BP3, BP4, and BP5 (see Table 1). As mentioned in the preamble, there is a pronounced sample dependence in the experimental exponent values as well as a significant dependence on the width of the temperature range employed in the corresponding fit to the power law. We want to remark that measurements presented in this work were performed very close to T_c $(t > 0.9)$. All previous structural and transport analysis prove that the difference between the samples stem from its intergranular properties mostly associated with an increase in the degree of texture with increasing the uniaxial compacting pressure.

It is important to notice that values of $n \sim 2$ very close to T_c indicate a SNS grain-boundary type as suggested above [1, 5, 6, 22].

In order to gain further information regarding the coupling between grains in our samples, we have also investigated the product $J_c\rho_{sr}$ in the uniaxially pressed samples. Table 1 displays the obtained values at $T = 0.96T_c$ for samples BP2, BP3, BP4, and BP5. An appreciable rise of ∼5 times between the outermost samples can be observed with increasing the uniaxial compacting pressure. In this case, typical values at $T = 4.2$ K in high-T_c materials are in the range 1–3 mV. However, a reduction of two or three orders of magnitude are expected as the temperature approaches to T_c. Thus, although is noticeable the very low values of the product $J_c\rho_{sr}$ in our samples the results seems to be adequate. Usually, the small value of $J_c\rho_{sr}$ can be interpreted as gap suppression at the boundary [1]. Leaving aside the temperature effect, the observed increase in the product $J_c\rho_{sr}$ indicates an improve of the grain connectivity, which also enhance the magnitude of the order parameter across the junction. In samples studied in this work, such a behavior is owed to the direct relation between the product $J_c\rho_{sr}$ and the grain-boundary orientation, θ. All previous analyzes indicate that increasing the uniaxial compacting pressure provokes an increase in the degree of texture of samples (see also Ref. [15]). In this sense is also expected a decrease in the θ. Such a behavior in combination with the different θ dependencies of J_c and ρ_{sr} [7, 8], favor the observed increase in the product $J_c\rho_{sr}$. Notice that, while J_c is reduced with increasing θ, the specific resistance rises almost in the same magnitude as reported elsewhere [7].

4 Conclusions

In summary, we have studied systematically the influence of the uniaxial compacting pressure on the granular structure $Bi_{1.65}Pb_{0.35}Sr_2Ca_2Cu_3O_{10+\delta}$ samples by means of transport measurements. The chemical composition of samples indicates that the majority phase correspond with the Bi-2223. Consequently, samples were found to have similar intragranular properties, but different intergranular features. Both electrical resistivity and critical current density as a function of temperature, respectively, was found strongly sensitives to the increase of the uniaxial compacting pressure. The above type of mechanical deformation improve the alignment of the grains perpendicular to the c-axis. As a consequence, samples exhibit an enhance in the intergranular properties, resulting in a decrease of the specific resistance of the grain-boundary and an increase in the critical current density. Finally, the product $J_c\rho_{sr}$ increase appreciably assuring an improve of the order parameter across the grain-boundaries.

Acknowledgements This work was supported by the Brazilian agencies Fundação de Amparo à Pesquisa do Estado de São Paulo (FAPESP) under Grant No. 05/53241-9 and Conselho Nacional de Desenvolvimento Científico e Tecnológico (CNPq) under Grant No. 473932/2007-5. One of us E.G.-A. acknowledges FAPESP under Grant No. 2009/51562-3. R.F.J. is CNPq fellow under Grant No. 308706/2007-2.

References

1. Hilgenkamp, H., Mannhart, J.: Grain boundaries in high-T_c superconductors. Rev. Mod. Phys. **74**, 485 (2002)
2. Darhmaoui, H., Jung, J.: Crossover effects in the temperature dependence of the critical current in $YBa_2Cu_3O_7$. Phys. Rev. B **53**, 14621 (1996)
3. Tinkham, M.: Resistive transition of high-temperature superconductors. Phys. Rev. Lett. **61**, 443 (1988)
4. Gross, R., Chaudhari, P., Dimos, D., Gupta, A., Koren, G.: Thermally activated phase slippage in high-T_c grain-boundary Josephson junctions. Phys. Rev. Lett. **64**, 228 (1990)
5. Prester, M.: Current transfer and initial dissipation in high-superconductors. Supercond. Sci. Technol. **11**, 333 (1998)
6. Babić, E., Prester, M., Drobac, D., Marohnić, Z., Biskup, N.: Intrinsic variation of the intergrain critical current in polycrystalline $YBa_2Cu_3O_{7-x}$. Phys. Rev. B **43**, 1162 (1991)
7. Hilgenkamp, H., Mannhart, J.: Superconducting and normal-state properties of $YBa_2Cu_3O_{7-\delta}$-bicrystal grain boundary junctions in thin films. Appl. Phys. Lett. **73**, 265 (1998)
8. Graser, S., Hirschfeld, P.J., Kopp, T., Gutser, R., Andersen, B.M., Mannhart, J.: What limits supercurrents in high temperature superconductors? A microscopic model of cuprate grain boundaries. To be published in Nat. Phys., available at arXiv:0912.4191v1
9. Govea-Alcaide, E., Jardim, R.F., Muné, P.: Correlation between normal and superconducting transport properties of $Bi_{1.65}Pb_{0.35}Sr_2Ca_2Cu_3O_{10+\delta}$ ceramic samples. Physica C **423**, 152 (2005)
10. Govea-Alcaide, E., García-Fornaris, I., Muné, P., Jardim, R.F.: Improvement of the intergranular pinning energy in uniaxially compacting $(Bi\text{-}Pb)_2Sr_2Ca_2Cu_3O_{10+\delta}$ ceramic samples. Eur. Phys. J. B **58**, 373 (2007)
11. Muné, P., Govea-Alcaide, E., Jardim, R.F.: Influence of the compacting pressure on the dependence of the critical current with magnetic field in polycrystalline $(Bi\text{-}Pb)_2Sr_2Ca_2Cu_3O_x$ superconductors. Physica C **384**, 491 (2003)
12. Pandey, D., Mahesh, R., Singh, A.K., Tiwari, V.S., Kak, S.K.: Preparation of nearly single phase 2223 in $Bi_{1.6}Pb_{0.4}Sr_2Ca_2Cu_3O_y$ composition by a semi-wet route using $Pb_{0.2}SrCa(CO_3)_{2.2}$ precursor. Physica C **184**, 135 (1991)
13. Giannini, E., Savysyuk, I., Garnier, V., Passerini, R., Toulemonde, P., Flükiger, R.: Reversible melting and equilibrium phase formation of $(Bi,Pb)_2Sr_2Ca_2Cu_3O_{10+\delta}$. Supercond. Sci. Technol. **15**, 1577 (2002)
14. Shamray, V.F., Mikhailova, A.B., Mitin, A.V.: Crystal structure and superconductivity of Bi-2223. Crystallogr. Rep. **54**, 584 (2009)
15. García-Fornaris, I., Muné, P., Suzuki, P.A., Alberteris-Campos, M., Jardim, R.F., Govea-Alcaide, E.: Experimental and theoretical study of transport properties in uniaxially pressed $(Bi,Pb)_2Sr_2Ca_2Cu_3O_{10+\delta}$ ceramic samples. Physica C **470**, 269 (2010)
16. Díaz, A., Maza, J., Vidal, F.: Anisotropy and structural-defect contributions to percolative conduction in granular copper oxide superconductors. Phys. Rev. B **55**, 1209 (1997)

17. Fujii, T., Watanabe, T., Matsuda, A.: Comparative study of transport properties of $Bi_2Sr_2Ca_2Cu_3O_{10+\delta}$ and $Bi_2Sr_2CaCu_2O_{8+\delta}$ single crystals. Physica C **357**, 173 (2001)
18. Fujii, T.: private communication
19. Currás, S.R., Veira, J.A., Maza, J., Vidal, F.: Critical current density versus normal-state resistivity in granular high-temperature superconductors with different average grain size. Supercond. Sci. Technol. **13**, 1005 (2000)
20. Russek, S.E., Lathrop, D.K., Moeckly, B.H., Buhrman, R.A., Shin, D.H., Silcox, J.: Scaling behavior of $YBa_2Cu_3O_7$ thin film weak links. Appl. Phys. Lett. **57**, 1155 (1990)
21. Dimos, D., Chaudhari, P., Mannhart, J.: Superconducting transport properties of grain boundaries in $YBa_2Cu_3O_7$ bicrystals. Phys. Rev. B **41**, 4038 (1990)
22. Steel, D.G., Hettinger, J.D., Yuan, F., Miller, D.J., Gray, K.E.: Electrical transport properties of [001] tilt bicrystal grain boundaries in $YBa_2Cu_3O_7$. Appl. Phys. Lett. **68**, 120 (1996)